# Left frontal white matter atrophy links to timing mechanisms relevant to apraxia of speech

[1, 2]Rose Bruffaerts, MD, PhD, [1]Jolien Schaeverbeke, PhD, [3]Manon Grube, PhD, [1]Silvy Gabel, MSc, [2]An-Sofie De Weer, MSc, [2]Eva Dries, MSc, [2]Karen Van Bouwel, MSc, [3]Timothy D Griffiths, MD, PhD, [4]Stefan Sunaert, MD, PhD, [1,2]Rik Vandenberghe, MD, PhD

[1]Laboratory for Cognitive Neurology, Department of Neurosciences, KU Leuven, Belgium; [2]Neurology Department, University Hospitals Leuven, 3000 Leuven, Belgium; [3]Institute of Neuroscience, Medical School, Newcastle University, Newcastle-upon-Tyne, UK; [4]Radiology Department, University Hospitals Leuven, 3000 Leuven, Belgium.

Corresponding author: Rose Bruffaerts, MD, PhD, Herestraat 49, 3000 Leuven, Belgium, rose.bruffaerts@kuleuven.be

Search terms: primary progressive aphasia, apraxia of speech, nonfluent variant, MRI, perceptual timing, rhythm

The authors declare no competing financial interests.

Funding: This work was supported by Federaal Wetenschapsbeleid [Belspo 7/11]; FWO [G0925.15] and KU Leuven [OT/12/097, C14/17/108]. RB is a postdoctoral fellow of the Research Foundation Flanders (FWO).

## Abstract

### Objective

In apraxia of speech (AOS), we observed impaired perceptual timing abilities, which lead us to propose a shared mechanism of impaired perceptual timing underlying impaired rhythm discrimination (perceptual processing) and AOS (motor speech output). Given that considerable white matter damage is observed in these patients, we investigate whether white matter changes are related to impaired rhythm processing as one possible mechanism underlying AOS.

### Methods

We applied deformation-based morphometry (DBM) and diffusion tensor imaging (DTI) in 12 patients with the nonfluent variant (NFV) of Primary Progressive Aphasia (PPA) with AOS, as well as 11 patients with the semantic variant and 24 cognitively intact mature controls.

### Results

Seventy-five percent of the patients with NFV displayed impaired rhythm discrimination. Severity of the rhythm discrimination impairment correlated with the patients' speech rhythm abnormality measured from connected speech samples. Moreover, left frontal white matter volume loss adjacent to the supplementary motor area (SMA) correlated with impaired rhythm processing. In addition, we obtained tract-based metrics of the left Aslant tract, which is typically damaged in the NFV. The structural integrity of the left Aslant tract also correlated with rhythmic discrimination abilities in the NFV.

### Conclusions

A colocalized and perhaps shared white matter substrate adjacent to the SMA is associated with impaired rhythm discrimination and motor speech impairments. This indicates that impaired perceptual timing may be one of the neurocomputational mechanisms underlying AOS. Our observation that regional variations in left frontal lobe atrophy are linked to the phenotypical heterogeneity in NFV may facilitate earlier diagnosis.

## Introduction

The nonfluent variant of Primary Progressive Aphasia (NFV) is characterized by apraxia of speech (AOS) or agrammatism[1]. NFV is phenotypically heterogeneous: impaired AOS and agrammatism can arise in combination or isolation and hence give rise to three subtypes: primary progressive apraxia of speech (ppAOS), progressive agrammatic aphasia or mixed agrammatism and AOS[2–4]. This heterogeneity suggests a diversity of underlying neuroanatomical substrates. Our study focuses on the in-depth characterization of the mechanism and substrates underpinning AOS. Grey matter atrophy is consistently found in NFV in the left opercular part (BA44) of the inferior frontal gyrus (IFG), insula, premotor and the supplementary motor areas (SMA)[1,5]. Involvement of the SMA and the left lateral superior premotor cortex is linked to ppAOS[2,6]. In ppAOS, neurodegeneration of the (pre)motor cortex is more focal compared to the widespread atrophy that extends to the frontotemporal regions in progressive agrammatic aphasia[3,4].

Neuropathologically, NFV is somewhat heterogeneous, with a dominance of tau pathology in up to 88% of patients (Progressive Supranuclear Palsy (PSP), Corticobasal degeneration (CBD) or Pick's disease). Sporadically, TDP43-proteinopathy or Alzheimer's disease is found in NFV[7–9]. Frontal white matter changes are more common in NFV caused by tauopathies[10], especially in CBD[11]. In-depth knowledge about the relation between phenotype, structural changes and neuropathology is lacking, whereas a better understanding of this relationship is necessary for targeted development of pharmacological and rehabilitation therapy. So far, neuroimaging studies have mainly focused on grey matter changes. White matter changes may also contribute to impaired speech production in NFV[12,13]. Here, we specifically test whether white matter changes in NFV relate to impaired non-linguistic processing using non-verbal rhythmic auditory stimuli that do not convey meaning. This is motivated by our finding that rhythm discrimination is significantly impaired in NFV with AOS[14]. Because

impaired rhythm discrimination co-occurred with AOS, we hypothesized that both deficits are related through a common impairment in a "temporal scaffolding mechanism", which structures input and output in time[14,15]. Our perceptual timing tasks untangle the processing of the lower-order (local) versus higher-order (global) temporal structure of acoustic stimuli. Clinically, patients with AOS do not have consistent problems producing individual phonemes, but have difficulties with the suprasegmental timing of their speech[16]. We postulate that the tasks indexing higher-order processing will be most relevant to AOS.

We have expanded our previously published dataset[14] to include 12 NFV patients who participated in volumetric imaging. We test the correlation between perceptual timing deficits and tensor-based deformations of the brain (deformation-based morphometry, DBM) and diffusion tensor imaging (DTI) to elucidate the neuroanatomical correlate of the hypothesized temporal scaffolding mechanism. We opted for DBM rather than voxel-based morphometry (VBM) because automated segmentation in regions of abnormal grey and white matter might be unreliable and because DBM allows visualization of changes in subcortical structures containing grey and white matter[17]. DBM is also easier to interpret than VBM since it reflects atrophy without inference from other pathological white matter changes. Furthermore, we complement DBM with DTI. DTI is sensitive to white matter damage caused by tau pathology[18,19] and DTI metrics may able to discriminate between tauopathy and TDP43-proteinopathy[20]. We focused on the left frontal Aslant tract, which connects BA44 to medial frontal areas including the SMA[21]. Damage of the left Aslant tract is considered specific for the NFV phenotype[13,22]. Since it connects IFG with SMA, which has been identified as a gray matter correlate of temporal regularity processing in NFV[23,24], the left Aslant tract might also play a role in temporal scaffolding. Our approach aims to clarify the relationship between AOS, rhythm discrimination, and their potentially overlapping anatomical substrate to elucidate the phenotypical heterogeneity in NFV.

# Methods

## Participants

The study was approved by the Ethics Committee, University Hospitals Leuven. All participants provided written informed consent in accordance with the Declaration of Helsinki. PPA patients were recruited via the memory clinic University Hospitals Leuven. A consecutive series of 38 patients who fulfilled the international consensus criteria for PPA[1] enrolled for the experiment (2011-2019). The first 23 patients were described in [14], and the same case numbers are used. Seven patients were excluded due to: hearing loss (n = 3); lack of ability to perform the experimental tasks due to disease severity (n = 2); lack of cooperation (n = 1); unique phenotype (foreign accent syndrome, n = 1). The remaining 31 patients were able to undergo the extensive testing and produce reliable data. Before enrollment, each patient was classified according to the 2011 recommendations[1]. The classification relied on the clinical evaluation by an experienced neurologist (R.V.), in combination with neurolinguistics assessment and clinical MRI, as well as, where available, [$^{18}$F]fluorodeoxyglucose PET ([$^{18}$F]-FDG PET), CSF biomarkers for Alzheimer's Disease and [$^{11}$C]-Pittsburgh compound B amyloid PET. Twelve cases were classified as NFV (Table 1), 11 as the semantic variant (SV), and 8 as the logopenic variant (LV). The LV group will not be discussed because of the smaller sample size compared to the NFV and SV groups. All NFV cases exhibited AOS and 5 patients (case 20-23 and 31) also displayed single-word comprehension deficits upon testing and would also fit the more recently described criteria for the "mixed variant"[25,26]. All patients received a volumetric MRI scan and 7 NFV and 7 SV DTI imaging. Twenty-nine healthy controls (15 male, age range 51-76, education range 9-22 years) performed the perceptual timing tasks, 24 received volumetric MRI and 20 DTI imaging. Hearing sensitivity was measured in all participants using a clinical Bekesy-type audiometer for frequencies of 0.25, 0.5, 1, 2, 4 and 8kHz, on the left and right ear. Impaired

pure-tone perception has been observed in NFV[27], but here we included only participants able to detect stimuli of up to 1000 Hz below a hearing level of 30 dB on at least one side (Fig. 1). Controls, NFV and SV were matched in terms of age, gender, education or better-ear mean score (one-way ANOVA all P>0.136).

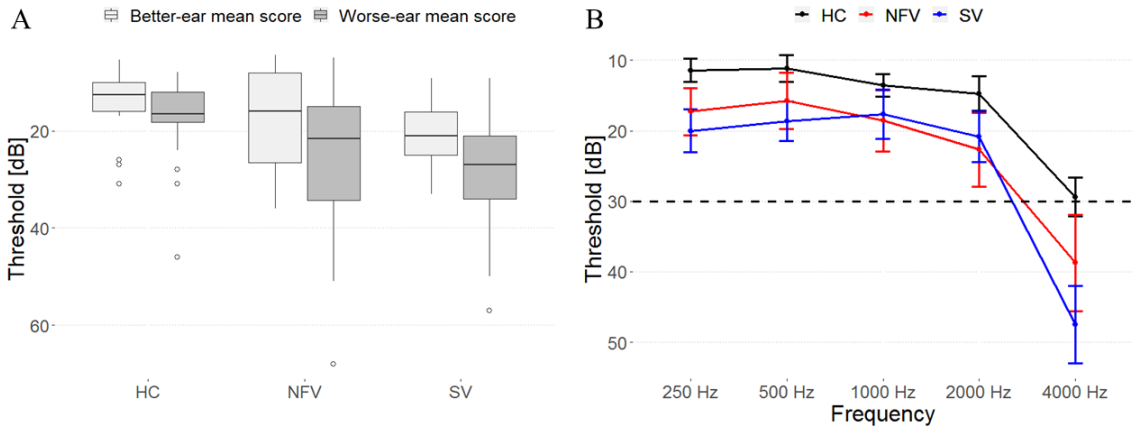


*Figure 1: Pure-tone audiograms of all participants. A) Mean composite ear and frequency score (250-4000 Hz) data for each participant group. B) Mean thresholds (and standard error of the mean) for detection of tones at frequencies of 250, 500, 1000, 2000 and 4000 Hz for each participant group.*

## Behavioral testing

Confrontation naming was tested using the Boston Naming test (Dutch norms). Non-verbal executive functioning was evaluated using Raven's Coloured Progressive Matrices. Speech repetition was assessed using the Akense Afasie test. To assess AOS, the Diagnostisch Instrument voor Apraxie van de Spraak (DIAS) was added when it became available (for this reason it was not performed in 4/12 cases). The DIAS consists of vowel and consonant repetition (15 trials each) and diadochokinesis testing. During the latter task, the examiner

first reads three successive alternating syllables aloud, e.g., "pa ta ka" and asks the patient to repeat these. If successful, he/she was asked to repeat it as many times as possible during a period of 8 s. The diadochokinesis severity score is the sum of correctly repeated syllables across trials. Grammaticality was assessed using the auditory sentence comprehension test of the Werkwoorden en Zinnen Test (WEZT), consisting of 40 sentence-picture matching trials with active or passive sentences containing possible role reversal (e.g. "the horse was kicked by the cow").

## Connected speech analysis

To obtain a measure of speech rhythm, we determined the normalized pairwise variability index (PVI) in connected speech samples using Praat 6.1.02. The samples consisted of a 2-minute "Cookie Theft Scene" description (20 controls, 11 NFV, 9 SV). For every participant, the median PVI[28] was determined for polysyllabic words with a strong-weak stress pattern (e.g. COO-kie) and for words with a weak-strong stress pattern (e.g. out-DA-ted). PVI was calculated following the procedure outlined in [28], equaling 100 x (d1 - d2)/ [(d1 + d2)/2], where d1 and d2 are the durations of the first and second vowel. Normalization corrects for a difference in speech rates. PVI is a marker of the suprasegmental timing of speech. PVI values closer to zero are consistent with relatively equal stress between the first two vowels of a word ("low contrastiveness")[28].

## Perceptual timing tasks

Testing comprised four pre-existing tasks of perceptual timing (r1-r4)[14](Fig 2A). The tasks followed a two-alternative forced-choice algorithm. Participants responded verbally or by pointing to a graphical scheme. Instructions, verbally and graphically, were repeated until the participant understood the task. Five practice trials were repeated until five consecutive

correct responses were recorded, and if needed, instructions were repeated and the nature of the errors was explained. If the participant indicated during the test phase that they had forgotten the instructions, then they were repeated, the practice trials run again and the test phase then restarted.

All tasks used 500Hz 100 ms pure tones and consisted of 50 trials. Outcome measures were the thresholds obtained by adaptively adjusting the difference between reference and target. The difference was varied as a relative proportion of the duration or tempo of the reference. The 'Single time-interval duration discrimination' task (r1) required participants to indicate which of two tone pairs comprised the 'longer gap'. Initially, the target was longer by 90% of the reference inter-onset-interval (depending on the trial, between 300 and 600 ms), and adaptively adjusted in steps of 12% and 6%. In the 'Isochrony deviation detection' task (r2), participants were required to indicate which of two otherwise isochronous five-tone sequences contained a lengthening or 'extra gap'. The reference sequence had an isochronous inter-onset-interval ranging from 300 to 600 ms. The target had one lengthened inter-onset-interval between the third and fourth tone. The initial default value of the lengthening was 60% of the inter-onset-interval, adaptively adjusted in steps of 6% and 2%. In both tasks (r1,r2), a local deviation is introduced to generate the target. As such, these tasks test the detection of lower-order differences in timing between consecutive tones. In the 'Metrical pattern discrimination' tasks (r3, r4), participants had to decide which of three rhythmic sequences (the second or the third) of seven tones sounded "different", based on a distortion within the rhythm. The reference sequence had a strongly (r3) or a weakly (r4) metrical beat of four evoked by the temporal spacing of the tones over 16 time units. In the strongly metrical sequence, accented tones occurred every four units, in the weakly metrical sequence, two of those were silent[29]. The default initial distortion in pattern (a change in the long compared to the short intervals) was 65%, adaptively adjusted in steps of 12% and 6%. Metrical pattern

discrimination (r3,r4) requires processing of the higher-order temporal structure of the stimuli, since global deviations distributed across the sequence need to be detected. Typical syllable rates in Dutch (the native language of the participants) are 4-5 syllables/s (period 200 – 250ms) which is close to the tempi used in our tasks.

## Statistical analysis

The analysis of the perceptual timing tasks was identical to [14]. Outcome measures were log-transformed to allow for parametric analysis at the group level. At the individual level, each patient's performance was analyzed in comparison to the group by using a modified Crawford *t*-test[30]. For the comparison between each patient and the controls, to facilitate comparison between tasks and to enable Bonferroni correction, the exact P values (estimated percentiles) calculated according to Crawford and Garthwaite were transformed into normalized Z-scores using the standard normal cumulative distribution function. The significance threshold was set to Z = 2.24 equaling a one-tailed significance level of $P<0.05$, Bonferroni-corrected for the number of tests (n = 4). We compared the thresholds between NFV and SV using a Student's *t*-test (one-tailed significance level of $P<0.05$, effect size: Cohen's d with Hedges correction for small samples, R package effsize). For NFV, SV and controls, we correlated PVI for strong-weak and weak-strong words to the perceptual timing tasks to test the link between impaired rhythm discrimination and speech rhythm (one-tailed significance level of $P<0.05$). We report the coefficient of determination ($R^2$) as well.

## Acquisition of MRI data

Twenty-three patients (12 NFV, 11 SV), and 24 controls received a high resolution T1-weighted structural MRI. All controls and 13 patients were scanned on a 3T Philips Intera

system equipped with an 8-channel receive-only head coil (SENSitivity Encoding head coil). Ten patients were scanned on a 3T Philips Achieva dstream scanner equipped with a 32-channel head volume coil. An identical 3D turbo field echo sequence was used on both systems (coronal inversion recovery prepared 3D gradient-echo images, inversion time (TI) 900 ms, shot interval = 3000 ms, echo time (TE) = 4.6 ms, flip angle 8°, 182 slices, voxel size 0.98x0.98x1.2 $mm^3$). The diffusion weighted images consisted of 45 directions of diffusion weighting with a b = 800 as well as 1 non-diffusion weighted image (B0), acquired in the axial plane, with isotropic voxel size of 2.2 mm, TR 9900 ms, TE 90 ms, flip angle 90°, fold over direction AP, fat shift direction A (anterior), in-plane parallel image acceleration (SENSE) factor 2.5.

## Deformation-based morphometry

DBM was performed using the CAT12 toolbox (http://www.neuro.uni-jena.de/cat), an extension of SPM12 (http://www.fil.ion.ucl.ac.uk/spm). Segmentation was performed in CAT12 using a default tissue probability map. Local adaptive segmentation was used at default strength (medium) and Diffeomorphic Anatomical Registration Through Exponentiated Lie Algebra (DARTEL) was used for registration to the default template (IXI555_MNI152). Voxel size for normalized images was set at 1.5 mm (isotropic) after internal resampling at 1mm. Local deformations were estimated using the Jacobian determinant, while ignoring the affine part of the deformation field. Thus, additional correction for total intracranial volume is not required[31]. Images were smoothed using a 8 x 8 x 8 $mm^3$ Gaussian kernel. Deformation fields of controls and both PPA groups were compared using a one-way between-subject ANOVA. Multiple linear regression was used to correlate tests (r1-r4) at the individual level to the deformation fields within each PPA subtype. Scanner type and age were introduced as nuisance variables in all analyses.

Threshold of significance was set at voxel-level uncorrected P<0.001 and cluster-level FWE-corrected P<0.05[14].

## Diffusion Tensor Imaging

Diffusion images were preprocessed and analyzed with MRTRIX3. The preprocessing pipeline included the following steps: first, the data were converted to MIF using mrconvert. Using dwidenoise, diffusion data were denoised; subject motion, and eddy current artefacts were also corrected for using dwidenoise (which relies on FSL eddy); following these two steps, the preprocessed diffusion data were bias-corrected with dwibiascorrect. The diffusion data were rigidly aligned to the subject's T1-weighted volume space using Advanced Normalization Tools (ANTs) and tensor reorientation was performed. Fractional anisotropy (FA) and mean diffusivity (MD) were calculated in subject-space and normalized to MNI space. The calculated tensors were then used to perform a whole brain tractography using the probabilistic Tensor (Tensor_Prob), combined with anatomically constrained tractography with seeding along the grey/white matter interface, and 2 million streamlines to be selected[32]. The whole brain tractogram was then segmented using volumes of interest (VOIs) acquired from the Freesurfer aparc+aseg parcellation[33,34]. These VOIs were pars opercularis of the IFG and the superior frontal gyrus, specifically selecting the Aslant tract on diffusion MR data[21].

Freesurfer aparc+aseg parcellation was performed to obtain these subject-specific VOIs. For this reason preprocessing of T1-weighted structural MRIs was repeated using FMRIPREP[35], a Nipype[36] based tool. T1-weighted volume was corrected for intensity non-uniformity using N4BiasFieldCorrection v2.1.0[37] and skull-stripped using antsBrainExtraction.sh v2.1.0 (using the OASIS template). Brain surfaces were reconstructed using recon-all (FreeSurfer v6.0.1[38]), and the brain mask estimated previously was refined with a custom variation of the method to

reconcile ANTs-derived and FreeSurfer-derived segmentations of the cortical gray matter[39]. Spatial normalization to the ICBM 152 Nonlinear Asymmetrical template version 2009c was performed through nonlinear registration with the antsregistration tool of ANTs v2.1.0 using brain-extracted versions of both the T1-weighted structural MRI and the template. Brain tissue segmentation of cerebrospinal fluid, white matter and gray matter was performed on the brain-extracted T1-weighted structural MRI using fast (FSL v5.0.9).

Smoothed FA and MD maps were compared between controls, NFV and SV using a between-subject ANOVA (same as previous threshold). Scanner type, TIV and age were introduced as a nuisance variables. A template for the left Aslant tract was generated for healthy controls using the 75% overlap threshold[21]. FA and MD of the left Aslant tract were extracted for each patient by averaging values from all voxels included in this template[21]. We compared the FA and MD between NFV and SV by means of a Student's t-test (one-tailed $P<0.05$). FA and MD were correlated to rhythm discrimination performance within the NFV group to confirm the DBM findings (one-tailed $P<0.05$).

## Data availability

The data that support the findings of this study are available upon reasonable request.

# Results

## Perceptual timing

Performance on the perceptual timing tasks was poorer in NFV compared to controls (Fig 2AB): mean Z scores were above the threshold (P<0.05 Bonferroni-corrected) in NFV for discrimination of strongly metrical sequences (r3, mean Z: 2.94), discrimination of weakly metrical sequences (r4, mean: 2.93) and isochrony deviation detection (r2, mean: 2.46) (Fig 2B). We compared the test scores between the NFV and SV. This resulted in significantly poorer scores in NFV for the discrimination of weakly metrical sequences (r4, P = 0.001, Hedges' g: 1.48) (Fig 2BC).

At the individual level, deficits were observed mainly in NFV patients (Z > 2.24) (Fig 2D). The weakly metrical pattern discrimination task (r4) resulted in a significant impairment in 7 NFV (Fig 2D) and 2 SV patients. Similarly, strongly metrical pattern discrimination (r3) was impaired in 6 NFV (Fig 2D) and 4 SV, as well as isochrony deviation detection (r2) in 6 NFV and 2 SV patients. Single time-interval discrimination (r1) was impaired in just 4 NFV and 1 SV patients. In summary, 75% of NFV cases were impaired in one or more of the tasks and 36.4% of SV cases.

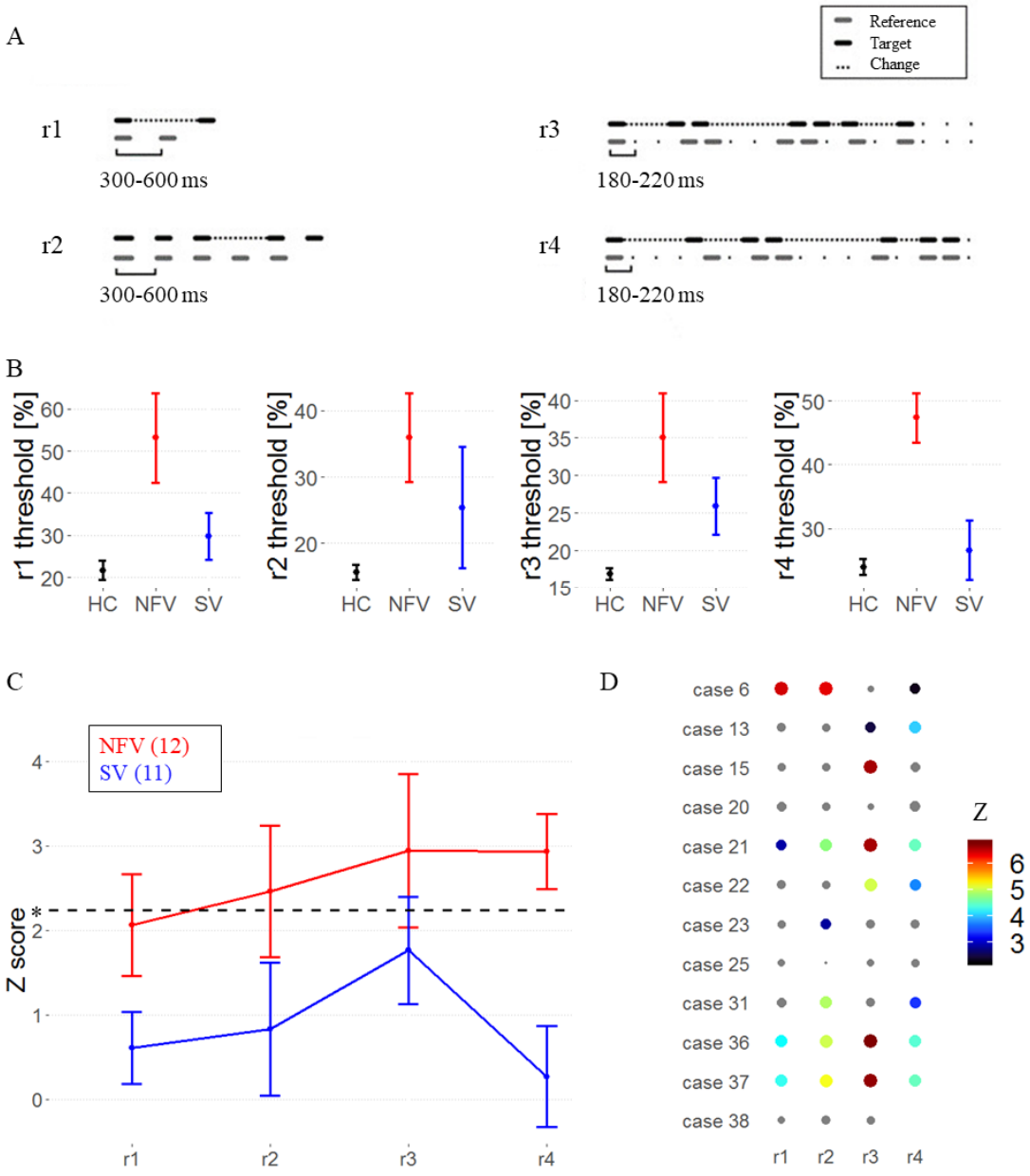


*Figure 2: Perceptual timing tasks A) Experimental design. B) Mean raw thresholds (and standard error of the mean) across controls, NFV and SV patients. C) Mean Z scores (and standard error of the mean) across PPA subtypes. Dotted line represents the Z cut-off for Bonferroni-corrected P<0.05. D) Z-scores of rhythm tests in NFV (case numbers refer to table 1). The size and color of dots reflect z-score value, non-significant values are gray. Missing data indicates that the patient was unable to perform the task.*

## Correlation with speech rhythm

PVI values were closer to zero ("low contrastiveness") for words with a weak-strong stress pattern in NFV compared to controls and SV (one-way ANOVA $F(2,35)=5.37$, $P = 0.009$, Fig 3A). PVI for strong-weak words correlated with strongly metrical pattern discrimination (r3) for NFV ($R = 0.634$, $R^2 = 0.402$, $P = 0.036$, Fig 3B), SV ($R = 0.761$, $R^2 = 0.579$, $P = 0.017$) and controls ($R = 0.531$, $R^2 = 0.282$, $P = 0.016$, Fig 3C). This means that participants with less accurate rhythm discrimination, displayed greater duration differences between the first and second vowels of words with a strong-weak stress pattern. No correlation was found with any of the other perceptual timing tasks (r1,r2,r4) and no correlation was found with the PVI for weak-strong words (all $P>0.1$).

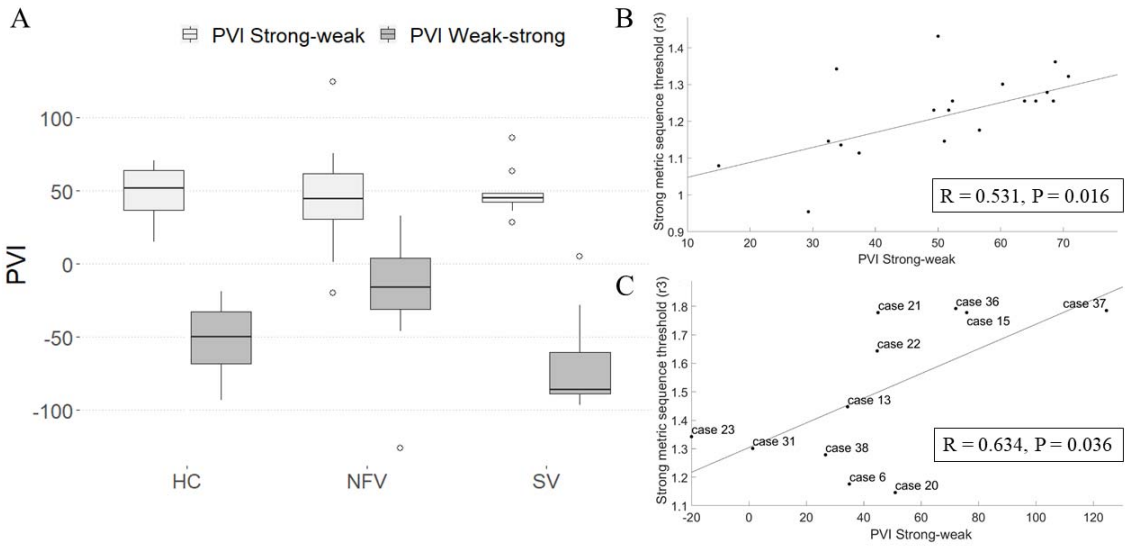


*Figure 3: Speech rhythm. A) Median PVI values for strong-weak and weak-strong words in the 3 participant groups. Correlation of PVI for strong-weak words and strong metric sequences threshold (r3, log-transformed) in B) healthy controls and C) the NFV patients (case numbers refer to table 1).*

## White matter changes: deformation-based morphometry

The expected pattern of changes of the deformation field was observed when comparing the healthy control, NFV and SV groups. In NFV, atrophy was observed mainly in the frontal lobes, with a left-sided predominance (Fig 4AB). In SV, atrophy was localized to the anterior temporal lobes (Fig 4A). In the NFV group, voxel-wise multiple linear regression showed that the strongly metrical rhythm discrimination task (r3) negatively correlated with changes in the deformation field in the left frontal white matter (MNI = -20,20,-36; -17,8,48; -9,39,50; $k_E$ 2426 voxels, Z score: 4.92) (Fig 5AB). This negative correlation indicates that poorer discrimination (i.e. larger thresholds and z scores) is linked to more atrophy. For illustrative purposes, we plotted the individual NFV thresholds for the strongly metrical discrimination task (r3) versus volume loss in this region ($R = -0.316$, $R^2 = 0.100$, $P < 0.001$) (Fig 5C). In the SV group, DBM analysis yielded no significant correlations with the perceptual timing tasks.

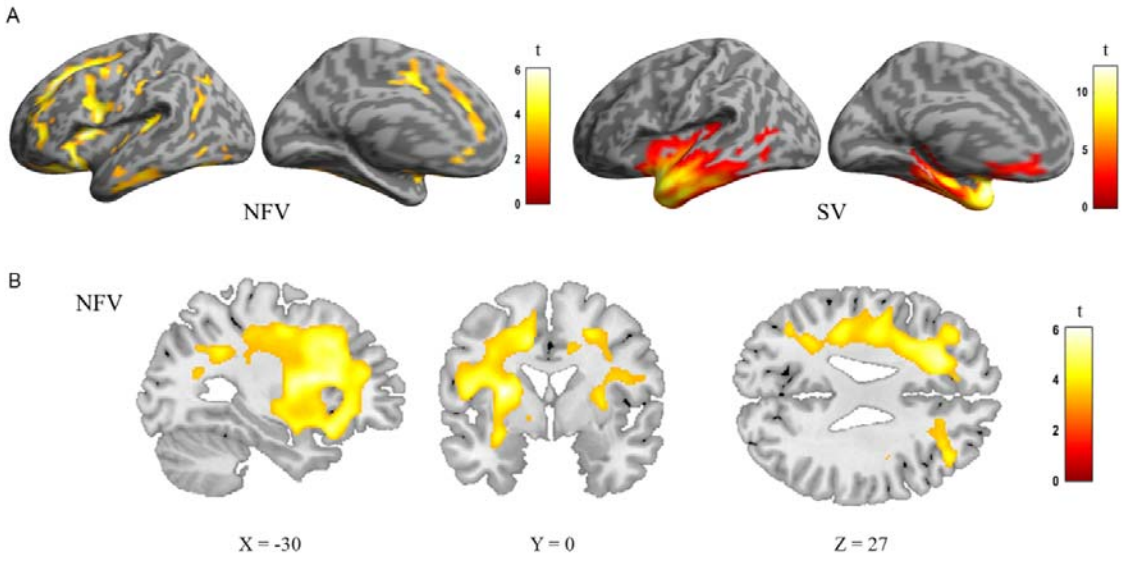

*Figure 4: DBM analysis: comparison of controls, the NFV and SV patients. A) Renderings shows deformation of 12 NFV and 11 SV compared to 24 controls (cluster-level FWE-corrected P<0.05). B) Slices in NFV*

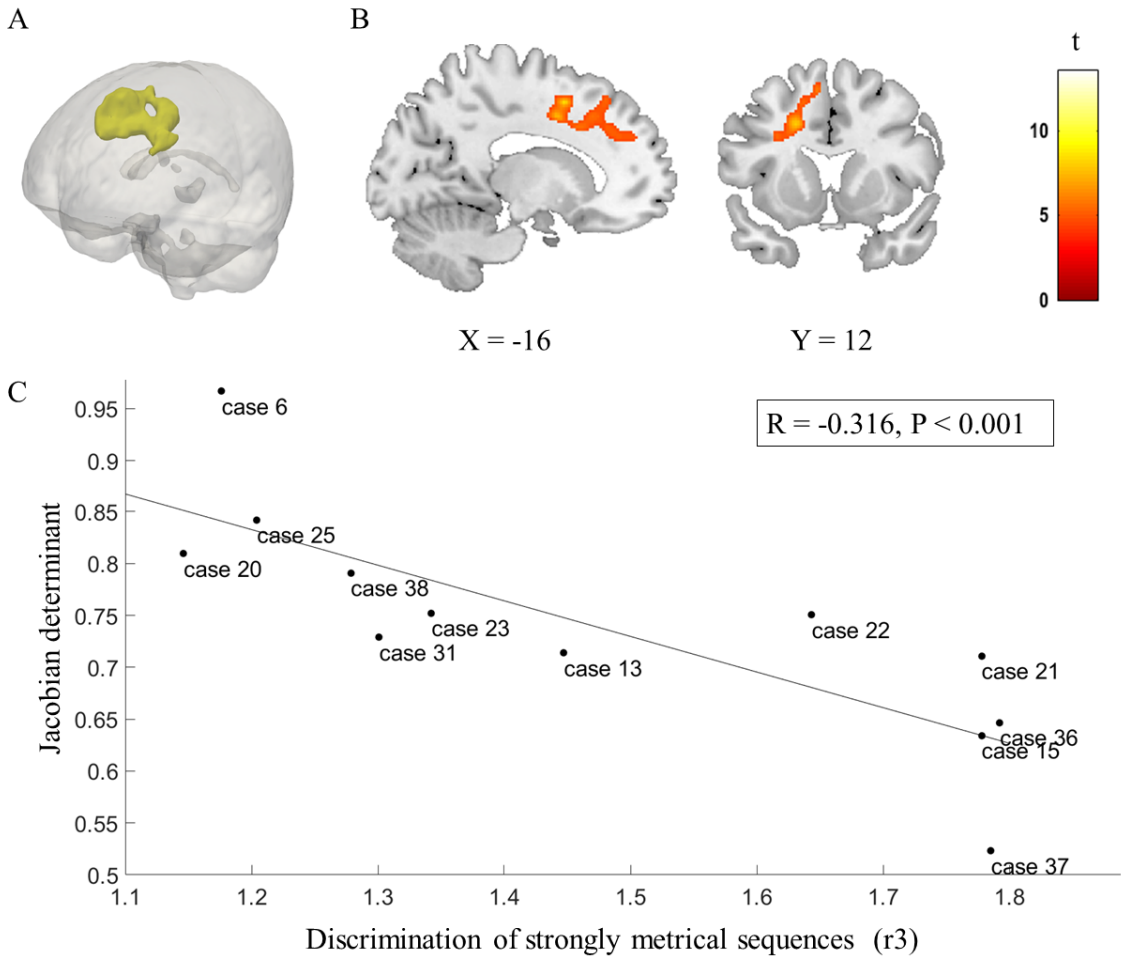


*Figure 5: DBM of strongly metrical sequence in NFV patients. A) Group rendering B) Slices C) Correlation between volume loss and strongly metrical sequence thresholds (r3, log-transformed) in NFV patients in the region of interest (AB), exploratory plot for illustrative purposes (case numbers refer to table 1)*

## White matter changes: Diffusion Tensor Imaging

A comparison between NFV, SV and controls showed reduced FA in NFV in the left inferior frontal region, the corpus callosum and the anterior cingulate (Fig 6A). MD was widely increased in NFV, with a predominance in both frontal lobes (Fig 6B). In SV, FA was reduced and MD was increased in both anterior temporal lobes (not shown). We then compared FA and MD between NFV and SV specifically within the template of the left Aslant tract derived from the controls. Although, FA was similar between NFV and SV (P=0.175, Hedges' g: -0.72, Fig 6C), MD was higher in NFV compared to SV (P = 0.038, Hedges' g: 1.17, Fig 6D). In NFV, MD in the left Aslant tract was increased when the performance on the strongly metrical rhythm discrimination task was weaker (r3) ($R = 0.815$, $R^2 = 0.664$, $P = 0.026$). Although this was not significant, a trend was observed with FA ($R = - 0.708$, $R^2 = 0.501$, $P = 0.075$). Neither FA nor MD in the left Aslant tract correlated with performance on any other task in NFV (r1,r2,r4, all P>0.231). Visual inspection of the left Aslant tract in NFV showed that this tract overlapped with the region where there were white matter volume changes identified by DBM (Fig 6E).

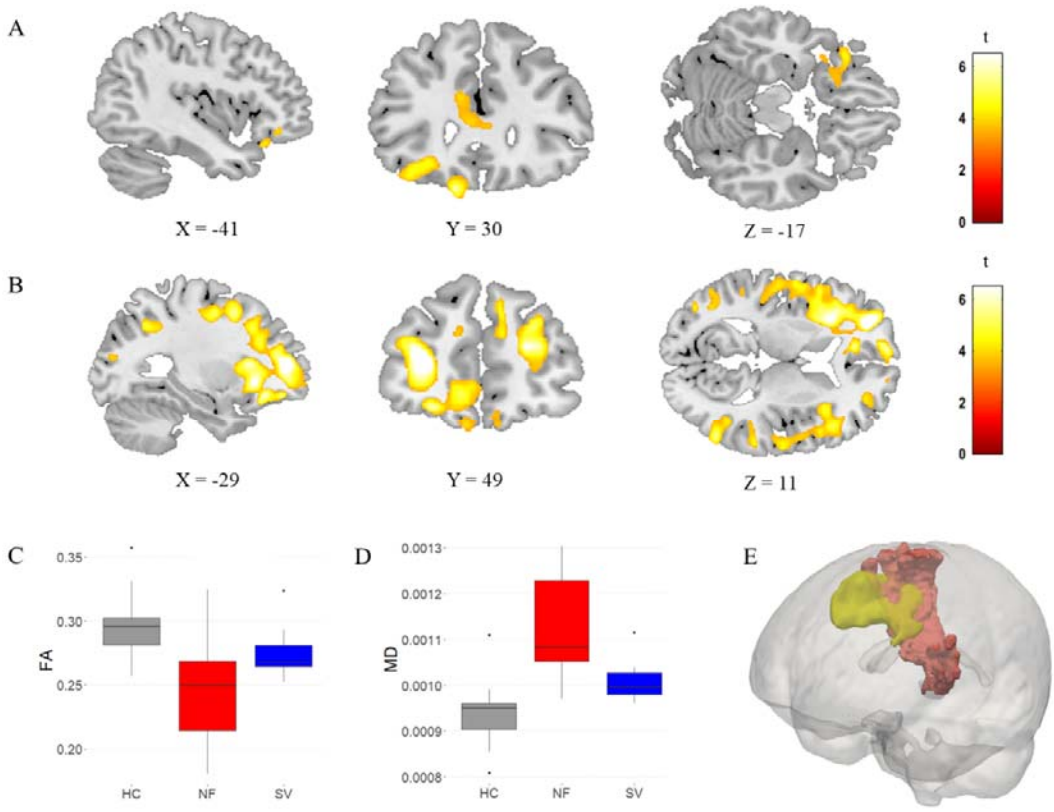


*Figure 6: DTI Metrics. A) FA in NFV patients versus controls (cluster-level FWE-corrected P<0.05). B) MD in NFV cases versus controls (cluster-level FWE-corrected P<0.05). Comparison of C) FA and D) MD in the left frontal Aslant tract between the NFV and SV subtypes and healthy controls (HC). E) Visualization of the Aslant tract in NFV, based on the 75% overlap of individual tracts in NFV (red) as well as the region of interest derived from DBM (yellow)*

## Discussion

By correlating white matter changes to perceptual timing impairments in AOS, we investigated the link between clinical heterogeneity and structural abnormalities in NFV. We propose a shared mechanism for impaired rhythm discrimination and AOS[14], whereby the impact of disrupted temporal scaffolding might well extend beyond the linguistic domain. Behaviorally, we observed a correlation between impaired rhythm discrimination and speech rhythm. DBM demonstrated that atrophy in the left frontal lobe correlated with the rhythm discrimination impairment in NFV. We complemented DBM with DTI to provide an independent measure of white matter changes. DTI confirmed a correlation between damage to the left Aslant tract and impaired rhythm perception in NFV. Our findings link impaired perceptual timing of incoming non-linguistic auditory signals to white matter atrophy in the left frontal lobe. Given the prior work implicating the left Aslant tract to motor speech production deficits in NFV[13,21,22], our results suggest it is a relevant (part of a) common anatomical substrate for impaired rhythm discrimination and AOS. Whilst our findings are correlational, the results for connected speech complement the two independent white matter metrics. This strengthens the evidence base for a well-defined neurocomputational mechanism of distorted speech. It provides insight into temporal irregularities in spontaneous speech patterns in AOS, as well as the critical role of left frontal regions in this process.

We observed an overlapping white matter substrate that might contribute to impaired rhythm discrimination as well as AOS. White matter degeneration was present in the left frontal Aslant tract close to the SMA, which has previously been linked to temporal regularity discrimination[24] and AOS[3,6]. The Aslant tract connects the superior frontal gyrus/SMA to the IFG, the region which displays the most pronounced atrophy in early NFV[40]. Agrammatism has been linked to grey matter damage in left BA44[41] and white matter damage in the adjacent left anterior inferior and middle frontal regions and uncinate fasciculus[4], which connects the

IFG to the temporal lobe[12,21]. The close anatomical proximity of the IFG and the left Aslant tract could explain why agrammatism and AOS often occur simultaneously in NFV, but also why these deficits can occur in isolation[42]. The clinical relevance of our study is the additional evidence for regional variations in left frontal lobe atrophy that is linked to the phenotypical heterogeneity in NFV.

Although four perceptual timing tasks were performed, both speech rhythm and left frontal lobe atrophy were linked specifically to impaired performance on the strongly metrical rhythm discrimination task (r3). This task is conceptually different from the single time-interval duration discrimination task (r1) and the isochrony deviation detection task (r2): determining the metricality of a tone sequence (r3) requires processing of the higher-order temporal structure determined by the grouping of salvos of notes that induce the sense of a regularly occurring metrical 'beat'[29]. Metricality-based rhythm discrimination (r3) necessitates detecting global deviations distributed across the entire sequence. The correlation between rhythm discrimination and speech rhythm may stem from the common processes required to integrate the higher-order/suprasegmental temporal structure. Our results are in agreement with prior work in PPA that demonstrates the detection of temporal changes between syllables was more impaired when stimuli contained a higher number of syllables[43]. In contrast, the single time-interval duration discrimination task (r1) and the isochrony deviation detection task (r2) test lower-order differences in timing in a simple isochronous sequence based on a local deviation. The weakly metrical rhythm discrimination task (r4) is more challenging as it does not rely on a clear metrical beat[29] (higher thresholds for r4 versus r3 in controls, $P<0.001$). Perhaps more domain-general processes play a role in this task, but additional manipulations are required to confirm this hypothesis. Keeping in mind the labor-intensive administration of our tasks, we reached a considerable albeit modest sample size. Further validation requires a larger multicentric sample given the relative rarity of PPA.

Performance on the strongly metrical rhythm discrimination task (r3) also correlated with the temporal variability in speech rhythm, strengthening the hypothesis that perceptual timing and AOS are linked. Similar to prior work, we observed lower contrastiveness of vowel duration in words with a weak-strong pattern[16,28]. Distortion of weak-strong words most likely reflects an early change in AOS secondary to abnormal lengthening of the first vowel[44]. Marked distortions of strong-weak words are more likely to occur when the disease is more severe[44]. Perhaps the overall low contrastiveness at the NFV group level for weak-strong words resulted in a floor effect, thus prohibiting us to detect a correlation with perceptual timing, whereas changes may be more subtle for strong-weak words. Future research on the physiological link between speech rhythm and perceptual timing might also include the use of delayed auditory feedback. This manipulation, consisting of delayed playback of the speaker's own voice, which elicits nonfluent speech in healthy participants, may improve speech in NFV patients[45].

White matter damage is at least part of the substrate of impaired rhythm discrimination and AOS in NFV. One question is whether these white matter changes reflect tau pathology, the most prevalent pathology in NFV[8,9]. DTI metrics have been put forward as a marker of tauopathy and other proteinopathies[46,47]. DTI imaging is sensitive to changes caused by tau pathology at the single-subject level[18], presumably because of underlying glial pathology[48], e.g. by myelin injury or changes in other structures that affect water diffusion[12]. Similar to prior work[49], we observed that MD changes were more pronounced than FA changes in NFV patients. In most patients, neuropathological data is lacking thus prohibiting us from making strong claims in relation to pathology. We would not advocate linking tauopathy to a simple DTI parameter. Rather, our findings advance the broader characterization of the possible disease-specific involvement of white matter tracts. Our results align with the "molecular nexopathy" paradigm[50]: the left frontal network containing IFG and SMA as nodes

demonstrate a selective vulnerability to tau protein, which could spread locally through the left Aslant tract in a prionlike fashion. Even if certain proteinopathies are strongly linked to predictable phenotypes of network disruption, the molecular nexopathy paradigm does not propose complete specificity. Furthermore, DBM demonstrated that the atrophy which correlated to impaired rhythm discrimination in NFV is more widespread than the left Aslant tract (Fig. 6E). The impact of these adjacent white matter changes remains unclear.

We revealed an overlap in the white matter substrates in rhythm processing of auditory input and suprasegmental timing of speech output. We thus present these correlates as the anatomical substrate of impaired temporal scaffolding and increase the mechanistic understanding of the origin of AOS. We also provide additional evidence that generic processing impairments explain part of the NFV phenotype.

## Acknowledgements

The authors thank B. Bergmans, MD, PhD, Ch. Swinnen, MD, A. Sieben, MD, and Y.A. Pijnenburg, MD, PhD, for the referral of patients. We thank E. Luckett, MSc, for copyediting.

# References

1. Gorno-Tempini ML, Hillis AE, Weintraub S, et al. Classification of primary progressive aphasia and its variants. Neurology. 2011;76:1006–1014.

2. Josephs KA, Duffy JR, Strand EA, et al. Characterizing a neurodegenerative syndrome: primary progressive apraxia of speech. Brain. 2012;135:1522–1536.

3. Tetzloff KA, Duffy JR, Clark HM, et al. Longitudinal structural and molecular neuroimaging in agrammatic primary progressive aphasia. Brain. 2018;141:302–317.

4. Tetzloff KA, Duffy JR, Clark HM, et al. Progressive agrammatic aphasia without apraxia of speech as a distinct syndrome. Brain. 2019;142:2466–2482.

5. Rogalski E, Cobia D, Harrison TM, et al. Anatomy of Language Impairments in Primary Progressive Aphasia. Journal of Neuroscience. 2011;31:3344–3350.

6. Whitwell JL, Duffy JR, Strand EA, et al. Distinct regional anatomic and functional correlates of neurodegenerative apraxia of speech and aphasia: an MRI and FDG-PET study. Brain Lang. 2013;125:245–252.

7. Harris JM, Gall C, Thompson JC, et al. Classification and pathology of primary progressive aphasia. Neurology. 2013;81:1832–1839.

8. Rogalski E, Sridhar J, Rader B, et al. Aphasic variant of Alzheimer disease. Neurology. 2016;87:1337–1343.

9. Spinelli EG, Mandelli ML, Miller ZA, et al. Typical and atypical pathology in primary progressive aphasia variants: Pathology in PPA Variants. Annals of Neurology. 2017;81:430–443.

10. Caso F, Mandelli ML, Henry M, et al. In vivo signatures of nonfluent/agrammatic primary progressive aphasia caused by FTLD pathology. Neurology. 2014;82:239–247.

11. Feany MB, Dickson DW. Neurodegenerative disorders with extensive tau pathology: a comparative study and review. Ann Neurol. 1996;40:139–148.

12. Galantucci S, Tartaglia MC, Wilson SM, et al. White matter damage in primary progressive aphasias: a diffusion tensor tractography study. Brain. 2011;134:3011–3029.

13. Canu E, Agosta F, Imperiale F, et al. Added value of multimodal MRI to the clinical diagnosis of primary progressive aphasia variants. Cortex. 2019;113:58–66.

14. Grube M, Bruffaerts R, Schaeverbeke J, et al. Core auditory processing deficits in primary progressive aphasia. Brain. 2016;139:1817–1829.

15. Bekius A, Cope TE, Grube M. The Beat to Read: A Cross-Lingual Link between Rhythmic Regularity Perception and Reading Skill. Frontiers in Human Neuroscience [online serial]. 2016;10. Accessed at: http://journal.frontiersin.org/Article/10.3389/fnhum.2016.00425/abstract. Accessed November 29, 2019.

16. Duffy JR, Hanley H, Utianski R, et al. Temporal acoustic measures distinguish primary progressive apraxia of speech from primary progressive aphasia. Brain Lang. 2017;168:84–94.

17. Cardenas VA, Boxer AL, Chao LL, et al. Deformation-Based Morphometry Reveals Brain Atrophy in Frontotemporal Dementia. Archives of Neurology. 2007;64:873.

18. Sajjadi SA, Acosta-Cabronero J, Patterson K, Diaz-de-Grenu LZ, Williams GB, Nestor PJ. Diffusion tensor magnetic resonance imaging for single subject diagnosis in neurodegenerative diseases. Brain. 2013;136:2253–2261.

19. Whitwell JL, Schwarz CG, Reid RI, Kantarci K, Jack CR, Josephs KA. Diffusion tensor imaging comparison of progressive supranuclear palsy and corticobasal syndromes. Parkinsonism Relat Disord. 2014;20:493–498.

20. McMillan CT, Irwin DJ, Avants BB, et al. White Matter Imaging Helps Dissociate Tau from TDP-43 in Frontotemporal Lobar Degeneration. J Neurol Neurosurg Psychiatry. 2013;84:949–955.

21. Catani M, Mesulam MM, Jakobsen E, et al. A novel frontal pathway underlies verbal fluency in primary progressive aphasia. Brain. 2013;136:2619–2628.

22. Mandelli ML, Caverzasi E, Binney RJ, et al. Frontal White Matter Tracts Sustaining Speech Production in Primary Progressive Aphasia. J Neurosci. 2014;34:9754–9767.

23. Hardy CJD, Agustus JL, Marshall CR, et al. Functional neuroanatomy of speech signal decoding in primary progressive aphasias. Neurobiology of Aging. 2017;56:190–201.

24. Hardy CJD, Agustus JL, Marshall CR, et al. Behavioural and neuroanatomical correlates of auditory speech analysis in primary progressive aphasias. Alzheimer's Research & Therapy [online serial]. 2017;9. Accessed at: http://alzres.biomedcentral.com/articles/10.1186/s13195-017-0278-2. Accessed February 11, 2019.

25. Mesulam M-M, Rogalski EJ, Wieneke C, et al. Primary progressive aphasia and the evolving neurology of the language network. Nat Rev Neurol. 2014;10:554–569.

26. Schaeverbeke J, Gabel S, Meersmans K, et al. Single-word comprehension deficits in the nonfluent variant of primary progressive aphasia. Alzheimer's Research & Therapy [online serial]. 2018;10. Accessed at: https://alzres.biomedcentral.com/articles/10.1186/s13195-018-0393-8. Accessed July 22, 2019.

27. Hardy CJD, Frost C, Sivasathiaseelan H, et al. Findings of Impaired Hearing in Patients With Nonfluent/Agrammatic Variant Primary Progressive Aphasia. JAMA Neurology. 2019;76:607.

28. Ballard KJ, Savage S, Leyton CE, Vogel AP, Hornberger M, Hodges JR. Logopenic and Nonfluent Variants of Primary Progressive Aphasia Are Differentiated by Acoustic Measures of Speech Production. Rodriguez-Fornells A, editor. PLoS ONE. 2014;9:e89864.

29. Grube M, Griffiths TD. Metricality-enhanced temporal encoding and the subjective perception of rhythmic sequences. Cortex. 2009;45:72–79.

30. Crawford JR, Garthwaite PH. Comparison of a single case to a control or normative sample in neuropsychology: development of a Bayesian approach. Cogn Neuropsychol. 2007;24:343–372.

31. Gaser C, Kurth F. Manual Computational Anatomy Toolbox - CAT12 [online]. 2019. Accessed at: http://www.neuro.uni-jena.de/cat12/CAT12-Manual.pdf.

32. Jones DK. Tractography gone wild: probabilistic fibre tracking using the wild bootstrap with diffusion tensor MRI. IEEE Trans Med Imaging. 2008;27:1268–1274.

33. Fischl B, van der Kouwe A, Destrieux C, et al. Automatically parcellating the human cerebral cortex. Cereb Cortex. 2004;14:11–22.

34. Desikan RS, Ségonne F, Fischl B, et al. An automated labeling system for subdividing the human cerebral cortex on MRI scans into gyral based regions of interest. Neuroimage. 2006;31:968–980.

35. Esteban O, Markiewicz CJ, Blair RW, et al. fMRIPrep: a robust preprocessing pipeline for functional MRI. Nature Methods. 2019;16:111–116.

36. Gorgolewski K, Burns CD, Madison C, et al. Nipype: A Flexible, Lightweight and Extensible Neuroimaging Data Processing Framework in Python. Frontiers in Neuroinformatics [online serial]. 2011;5. Accessed at: http://journal.frontiersin.org/article/10.3389/fninf.2011.00013/abstract. Accessed April 23, 2019.

37. Tustison NJ, Avants BB, Cook PA, et al. N4ITK: Improved N3 Bias Correction. IEEE Transactions on Medical Imaging. 2010;29:1310–1320.

38. Dale AM, Fischl B, Sereno MI. Cortical Surface-Based Analysis. NeuroImage. 1999;9:179–194.

39. Klein A, Ghosh SS, Bao FS, et al. Mindboggling morphometry of human brains. Schneidman D, editor. PLOS Computational Biology. 2017;13:e1005350.

40. Mandelli ML, Vilaplana E, Brown JA, et al. Healthy brain connectivity predicts atrophy progression in non-fluent variant of primary progressive aphasia. Brain. 2016;139:2778–2791.

41. Wilson SM, Dronkers NF, Ogar JM, et al. Neural correlates of syntactic processing in the nonfluent variant of primary progressive aphasia. J Neurosci. 2010;30:16845–16854.

42. Leyton CE, Ballard KJ, Piguet O, Hodges JR. Phonologic errors as a clinical marker of the logopenic variant of PPA. Neurology. 2014;82:1620–1627.

43. Rohrer JD, Sauter D, Scott S, Rossor MN, Warren JD. Receptive prosody in nonfluent primary progressive aphasias. Cortex. 2012;48:308–316.

44. Vergis MK, Ballard KJ, Duffy JR, McNeil MR, Scholl D, Layfield C. An acoustic measure of lexical stress differentiates aphasia and aphasia plus apraxia of speech after stroke. Aphasiology. 2014;28:554–575.

45. Hardy CJD, Bond RL, Jaisin K, et al. Sensitivity of Speech Output to Delayed Auditory Feedback in Primary Progressive Aphasias. Frontiers in Neurology [online serial]. 2018;9. Accessed at: https://www.frontiersin.org/article/10.3389/fneur.2018.00894/full. Accessed April 17, 2020.

46. Mahoney CJ, Malone IB, Ridgway GR, et al. White matter tract signatures of the progressive aphasias. Neurobiology of Aging. 2013;34:1687–1699.

47. Downey LE, Mahoney CJ, Buckley AH, et al. White matter tract signatures of impaired social cognition in frontotemporal lobar degeneration. NeuroImage: Clinical. 2015;8:640–651.

48. Forman MS, Zhukareva V, Bergeron C, et al. Signature tau neuropathology in gray and white matter of corticobasal degeneration. Am J Pathol. 2002;160:2045–2053.

49. Whitwell JL, Avula R, Senjem ML, et al. Gray and white matter water diffusion in the syndromic variants of frontotemporal dementia. Neurology. 2010;74:1279–1287.

50. Warren JD, Rohrer JD, Schott JM, Fox NC, Hardy J, Rossor MN. Molecular nexopathies: a new paradigm of neurodegenerative disease. Trends Neurosci. 2013;36:561–569.

# Tables

| **Case** | **6** | **13** | **15** | **20** | **21** | **22** | **23** | **25** | **31** | **36** | **37** | **38** | **Cut off** |
|---|---|---|---|---|---|---|---|---|---|---|---|---|---|
| Age | 52 | 79 | 71 | 78 | 72 | 63 | 62 | 57 | 69 | 58 | 80 | 65 | / |
| Gender | F | F | M | M | F | F | F | F | M | F | F | M | / |
| Education | 17 | 8 | 15 | 17 | 12 | 15 | 12 | 10 | 18 | 12 | 10 | 16 | / |
| CPM | 31 | **24** | **24** | 30 | **12** | 32 | 31 | / | 29 | **21** | **4** | 35 | <28 |
| Dis. Dur. | 2 | 5 | 1.5 | 2.5 | 2.5 | 5 | 2.5 | 3.5 | 1.5 | 4 | 4 | 3 | / |
| BNT | 58 | **48** | 55 | **48** | **30** | **41** | **46** | **7** | **29** | 52 | **27** | 57 | <50 |
| AAT rep 1 | 28 | 29 | 30 | 29 | **26** | 30 | 28 | **27** | **20** | 28 | **14** | 30 | <28 |
| AAT rep 2 | **26** | **24** | **21** | 30 | **28** | 30 | 30 | 29 | 30 | **28** | **25** | 30 | <29 |
| AAT rep 3 | **28** | **22** | 29 | **28** | **24** | 30 | 30 | **28** | 29 | **28** | **27** | 29 | <29 |
| AAT rep 4 | **26** | **23** | 30 | 29 | **24** | 30 | 29 | **15** | 29 | 28 | **14** | 30 | <28 |
| AAT rep 5 | **26** | **27** | 30 | 30 | **15** | 30 | 28 | **17** | 28 | **23** | **10** | 30 | <28 |
| DS | 6 | **3** | 4 | 6 | **2** | 4 | 5 | **3** | 7 | 5 | **3** | 4 | <4 |
| DIAS cons | / | / | / | **13** | / | 15 | **10** | 14 | **13** | **3** | **0** | 15 | <14 |
| DIAS vow | / | / | / | 15 | / | 15 | **14** | **14** | **14** | 15 | **6** | 15 | <15 |
| DIAS dia | / | / | / | 103 | / | 77 | **50** | **24** | 115 | **48** | **6** | **47** | <56 |
| Gramm | / | / | / | **36** | / | **35** | **36** | **29** | **31** | **20** | **11** | 38 | <38 |
| Extrapyr | - | - | + | - | - | + | + | + | + | - | - | - | / |
| CIT Spect | / | / | / | / | / | / | / | + | / | / | / | / | / |
| Tau CSF | / | 312 | / | 195 | **424** | 183 | / | 247 | / | 298 | 273 | **530** | >367 |
| Aβ42 CSF | / | 1028 | / | 816 | 1060 | 865 | / | 1057 | / | 1320 | 1264 | 1139 | <500 |
| Neuropath | / | CBD | CBD | / | / | / | / | / | / | / | / | / | / |

*Table 1. Characteristics of NFV patients. Norms were calculated as 2 standard deviations below the mean in the age- and education-matched group of healthy controls (n=29). CPM: Raven's progressive matrices, Dis. Dur.: disease duration (years), BNT: Boston Naming Test, AAT: Akense Afasie Test repetition scores part 1 to 5, DS: digit span forward, DIAS cons: DIAS repetition of consonants, DIAS vow: DIAS repetition of vowels, DIAS dia: DIAS diadochokinesis score, Gramm: grammaticality score WEZT, Extrapyr: extrapyramidal signs upon examination, Neuropath: anatomopathological findings*